Atomistic simulations of resistance to amorphization by radiation damage

Kostya Trachenko,* Martin T. Dove, and Emilio Artacho
Department of Earth Sciences, University of Cambridge, Downing Street, Cambridge CB2 3EQ, United Kingdom

Ilian T. Todorov and W. Smith
Computational Science and Engineering Department, CCLRC Daresbury Laboratory, Keckwick Lane, Daresbury, Warrington WA44AD, Cheshire, United Kingdom

(Received 7 November 2005; revised manuscript received 9 March 2006; published 10 May 2006)

We use molecular-dynamics simulations to study processes related to resistance to amorphization by radiation damage. We simulate high-energy radiation events in SiO_2, GeO_2, TiO_2, Al_2O_3, and MgO, and find that simulation results match the experiments. We discuss the difference between the damage that the structures along this series can support. We find that for the same material, activation barriers for damage recovery can strongly depend on the degree of structural damage. We observe that the effect of resistance to amorphization is primarily governed by the relaxation processes at the time scales of several picoseconds. On this time scale, we observe two distinct relaxation processes, reversible elastic deformation around the radiation cascade and recovery of the in-cascade damage of high topological disorder. Finally, we discuss how resistance to amorphization is related to interatomic interactions and to the nature of the chemical bond.

DOI: 10.1103/PhysRevB.73.174207 PACS number(s): 61.80.Az, 61.80.Jh

I. INTRODUCTION

Modification of materials by ion beams is a wide area in science and technology. A material is modified by the structural damage inflicted by an energetic particle which displaces atoms from their crystalline positions and creates a region of high structural disorder, "radiation cascade." Upon accumulation of these cascades, the long-range order in a material is lost, prompting the term radiation-induced amorphization. Experimentally, some materials are readily rendered amorphous, whereas others are very difficult or even impossible to amorphize by ion beams, i.e., are resistant to amorphization by radiation damage.[1] This leads to the question of what defines the ability to recover (recrystallize locally) from the damage, initially introduced by an energetic particle? Although many models have been discussed in the literature, they cannot be used to reliably predict resistance to amorphization,[1] begging the question of what is the main mechanism behind this phenomenon. A related interesting question is what are the important time scales of damage recovery in these materials. How does damage recovery during the cascade lifetime of several ps[2] compare to slow diffusive-type processes at the experimental time scale?[3] Answers to these questions are important for several practical applications, including the safe immobilization of highly radioactive nuclear waste. If a material in which nuclear waste is immobilized, becomes amorphized under irradiation (primarily by heavy recoils in alpha decay), it can show percolation-type increases of transport, which may lead to radioactive isotopes diffusing out in the environment.[4,5] A material resistant to amorphization, on the other hand, would be free from this negative effect.

A suitable tool to address these questions is molecular-dynamics (MD) simulation, in which an energetic particle is introduced in the structure and the phase trajectory of the damage is followed. These simulations model the processes of creation and evolution of radiation cascades on the scales of nanometers and picoseconds,[2] not accessible in the experiments. Unfortunately, small system size has often remained the limiting factor in these simulations. One needs to be able to simulate cascades produced by recoils of realistic experimental energies of at least several tens of keV. Depending on the material and ion type, the number of atoms in the MD box needed to contain the damage can exceed 1 million atoms, and when the force field includes electrostatics, a major factor behind the simulation slow-down, standard tools become impractical. We have recently developed the DL_POLY 3 MD package, based on the domain decomposition strategy, to simulate systems with millions of atoms with Coulomb interactions. Details of the method can be found in Ref. 6. For radiation damage simulations, we have made several adaptations, including scaling the energy at the (periodic) boundaries of the simulation box, fitting potentials at short distances to Ziegler-Biersack-Littmark repulsive interactions, and introducing variable time step.[6]

In this paper, we simulate high-energy events in several simple oxides in order to gain insights into the open questions above. We choose oxides as an interesting case study, because they show a very large difference in damage recovery.[1] We find that our simulations with empirical potentials reproduce experimental behavior of resistance to amorphization very well. We discuss the difference between the damaged structures along this series of materials and the meaning of the term "amorphous" when applied to a radiation cascade. We find that the degree of structural damage (amorphization) can profoundly affect activation barriers for damage recovery: the barriers increase as damage increases. Next, we find that resistance to amorphization by radiation damage is defined by relaxation processes that take place on the time scale of several picoseconds. On this time scale, we observe two distinct relaxation processes on this time scale, reversible elastic deformation around the radiation cascade, and recovery of the in-cascade damage of high topological disorder. Finally, we discuss how resistance to amorphization

is related to the details of interatomic potentials and to the nature of the chemical bond.

We simulate radiation cascades in SiO_2 (quartz), GeO_2 (quartz), rutile TiO_2, Al_2O_3 (corundum), and MgO. The reason for this choice of materials is that they cover a very wide range of resistance to amorphization by radiation damage, and hence by studying the evolution of radiation cascades in them we hope to find insights into the phenomenon of resistance. In addition, TiO_2 forms the base of the potential ceramic waste form, and has been investigated in this context.[1] A convenient measure of resistance is the critical amorphization temperature T_c, defined as the temperature above which no radiation-induced amorphization occurs; the lower T_c, the higher resistance. Experimental values of T_c are 1400 K for SiO_2,[7] 876 K for GeO_2,[8] 200 K for TiO_2,[9] 123 K for Al_2O_3,[7] and <20 K for MgO,[7] respectively. Hence at room temperature, SiO_2 and GeO_2 become amorphous, whereas Al_2O_3 and MgO remain crystalline by virtue of very efficient damage recovery. TiO_2 is perhaps in between the two cases since in some experiments it remains crystalline at room temperature,[9] and in others it can be amorphized, albeit at a very high radiation dose.[10]

We use empirical potentials for SiO_2,[11] GeO_2,[12] TiO_2,[13] and MgO.[14] For comparative purpose, we have used two different potentials for Al_2O_3 from Refs. 14 and 15 (without shells), denoted below as $Al_2O_3^{(1)}$ and $Al_2O_3^{(2)}$. All potentials consist of Coulomb and Buckingham pair interactions, with parameters derived by either fitting to the results of quantum-mechanical calculations or experimental data. We model radiation damage created by heavy recoils in alpha decay, a common decay process in highly radioactive nuclear waste responsible for radiation-induced amorphization, and simulate the propagation of the U atom. The U atom is given the energy of 40 keV. We use constant energy ensemble with scaled boundaries[6] at room temperature. Depending on a material, the number of atoms in MD simulation is 2–2.3 million atoms.

II. RADIATION CASCADES

A. Simulation and experiment

An energetic recoil displaces atoms from their equilibrium positions, which, in turn, displace other atoms, resulting in a highly disordered region, "radiation cascade." Radiation cascades in SiO_2, GeO_2, TiO_2, $Al_2O_3^{(1)}$, $Al_2O_3^{(2)}$, and MgO, shown in Figs. 1–6, can be easily seen as darkened regions due to high structural disorder, and are contrasted to the surrounding periodic crystalline lattice. In all materials, the direction of recoil atom is from the top left to the bottom right of the simulation box. In each of the Figs. 1–6, the top frame shows the damage at its peak (found by counting the displaced atoms, defined as atoms which travel more than half the nearest-neighbor distance), and the bottom frame shows damage relaxation to its final state. These figures show all atoms in the MD simulation box. We used the Atomeye tool for structure visualization.[16]

By analyzing Figs. 1–6, we conclude that our simulations generally reproduce experimental resistance to amorphization by radiation damage. We first note that cascade geometry is quite different in the five materials studied, due to the different structure and density. We observe that SiO_2 and GeO_2 show little damage recovery, as most of the created damage is stabilized after a few ps and does not change up to 50 ps (see Figs. 1 and 2). This behavior is consistent with experiments in which these materials are readily amorphized at room temperature.[7,8] Next, there is significant damage recovery in TiO_2 (see Fig. 3), consistent with experiments.[9] A small amorphous pocket is nevertheless left in the core of the damaged region. This suggests that at a very high dose, it is still possible to amorphize TiO_2 at room temperature, which is what is seen in the experiment.[10] Finally, almost perfect damage recovery is seen in $Al_2O_3^{(2)}$ and MgO (see Figs. 5 and 6), consistent with experiments,[7] although close inspection of the structure reveals the presence of point defects, which we will discuss below. One can conclude therefore that damage recovery in the simulation is generally consistent with experimental behavior. To show an exception to this trend, we have included the simulation of $Al_2O_3^{(1)}$ which apparently supports permanent damage of significant size (see Fig. 4). This difference with perfect damage recovery of $Al_2O_3^{(2)}$ (Fig. 5) is instructive and will be discussed below.

It is interesting to ask why MD simulations with empirical potentials generally give correct results of resistance to amorphization by radiation damage. Indeed, all empirical potentials are fitted to structure and elastic properties of materials at equilibrium. Radiation cascades, on the other hand, represent highly nonequilibrium processes, and one is led to ask why equilibrium-fitted potentials are so successful in describing highly nonequilibrium processes? It may be argued that potential curvature at equilibrium generally correlates with the height of activation barrier. A schematic argument suggests that the larger this curvature (corresponding to a stiffer local potential), the larger the activation barrier.[17] As we discuss below, it is this barrier that governs damage recovery and resistance to amorphization by radiation damage.

B. Some features of the damaged structures

Damage accumulation is often discussed in the literature as "amorphization." This includes numerous computer modeling work, in which the damage is introduced in one way or another, and the question is asked at which point a structure becomes amorphous. One can ask a similar question about the damaged structure in Figs. 1–6. Before discussing this point, we make two notes. First, the term "amorphous" implies the absence of the long-range order. Being quite general, this definition assumes the existence of many structures in which the long-range order is lost and which at the same time are quite different from each other. For example, a very common model for many glasses is the continuous random network, which is characterized by the full connectivity of short-range building blocks.[18] Assuming that a certain freedom exists in connecting these blocks (giving rise, for example, to the wide distribution of A-O-A angle a tetrahedral AO_2 glass structure), an (almost) stress-free continuous structure can be constructed. As such, this amorphous structure is expected to be quite different from the structure damaged by displacive radiation, which can contain high-energy

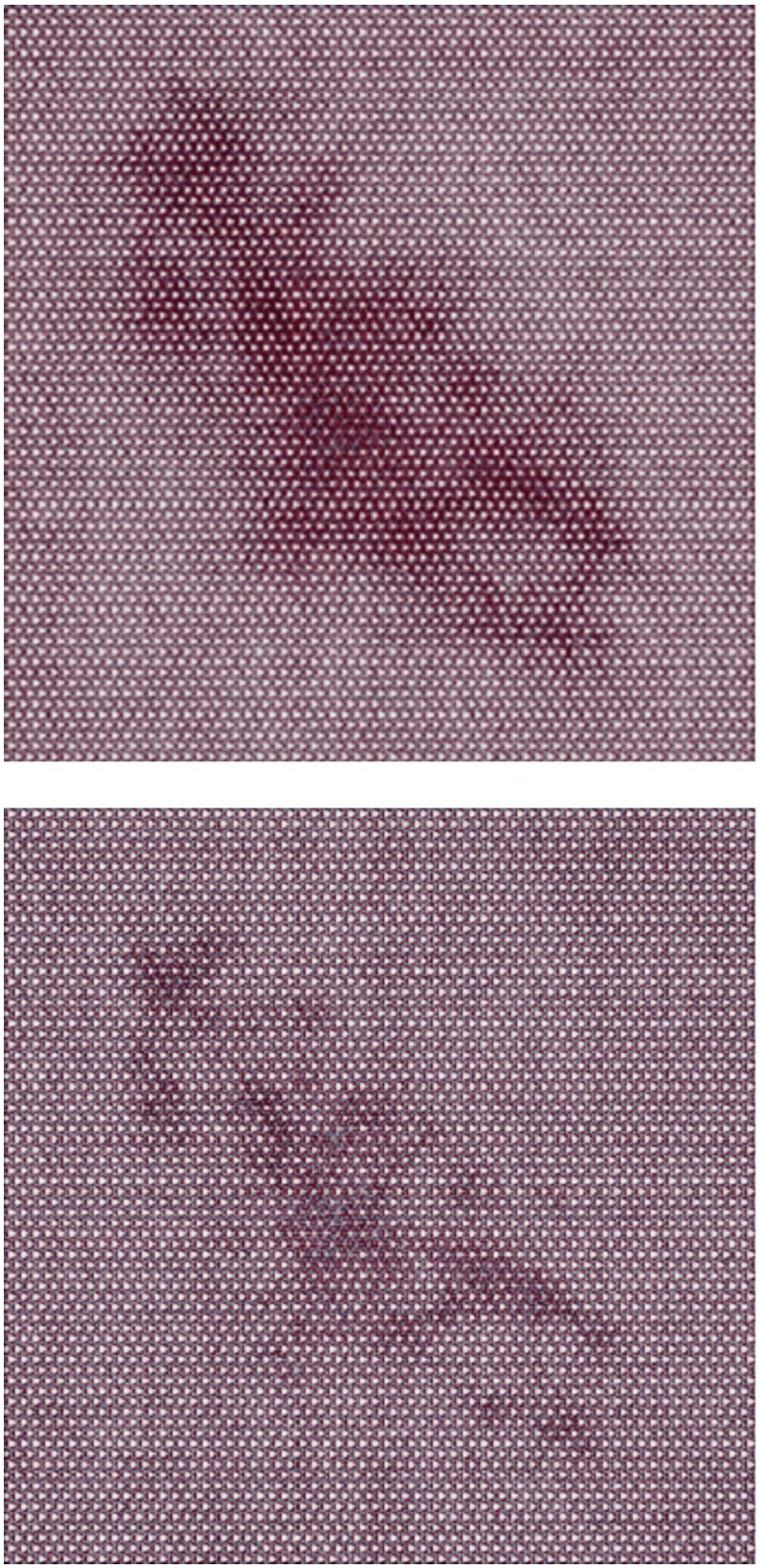

FIG. 1. (Color online) Radiation damage in SiO_2, showing the damage at its peak (top), and relaxed damage at the end of simulation (bottom). The size of MD simulation box is approximately 31 nm.

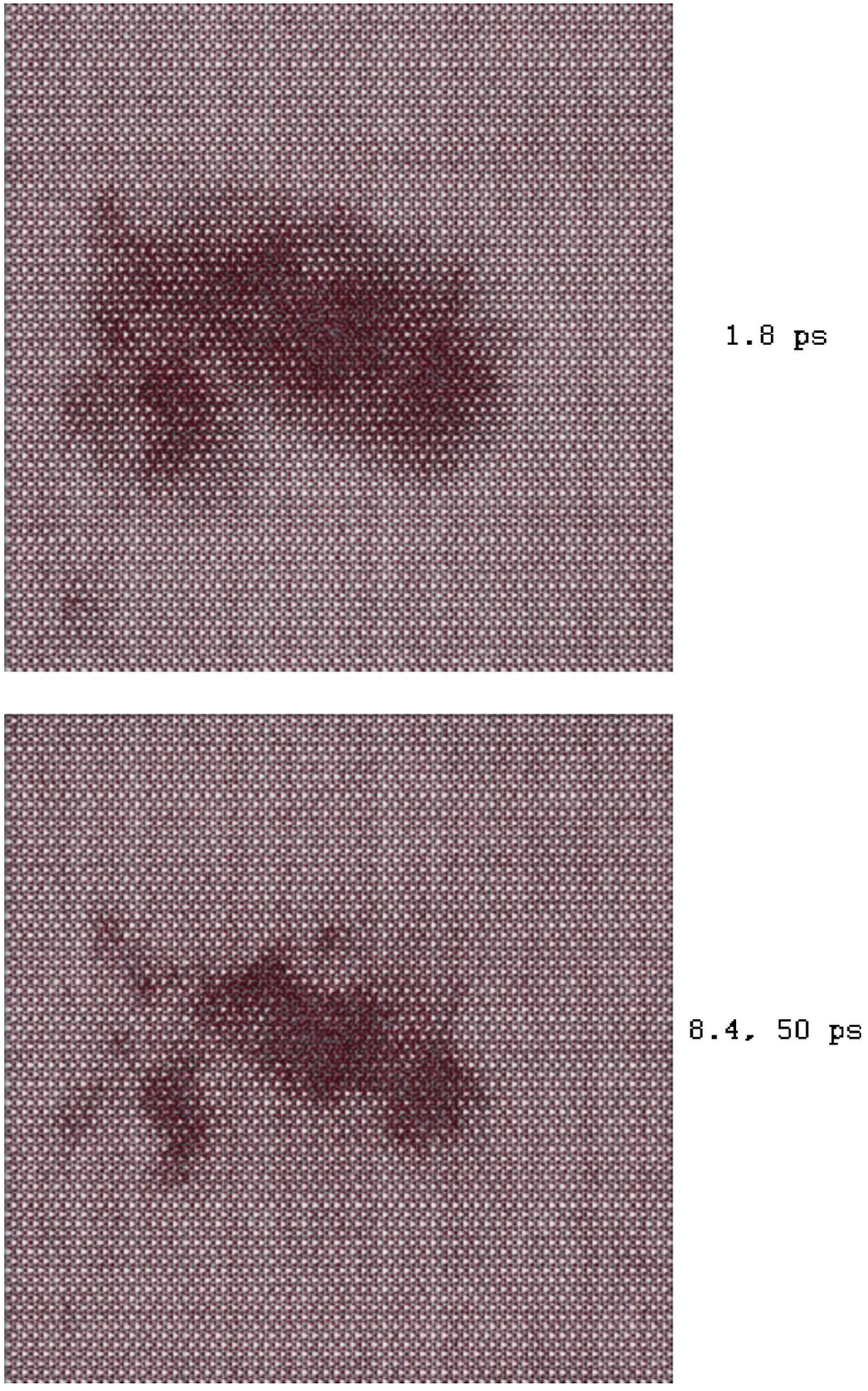

FIG. 2. (Color online) Radiation damage in GeO_2, showing the damage at its peak (top), and relaxed damage at the end of simulation (bottom). The size of MD simulation box is approximately 32 nm.

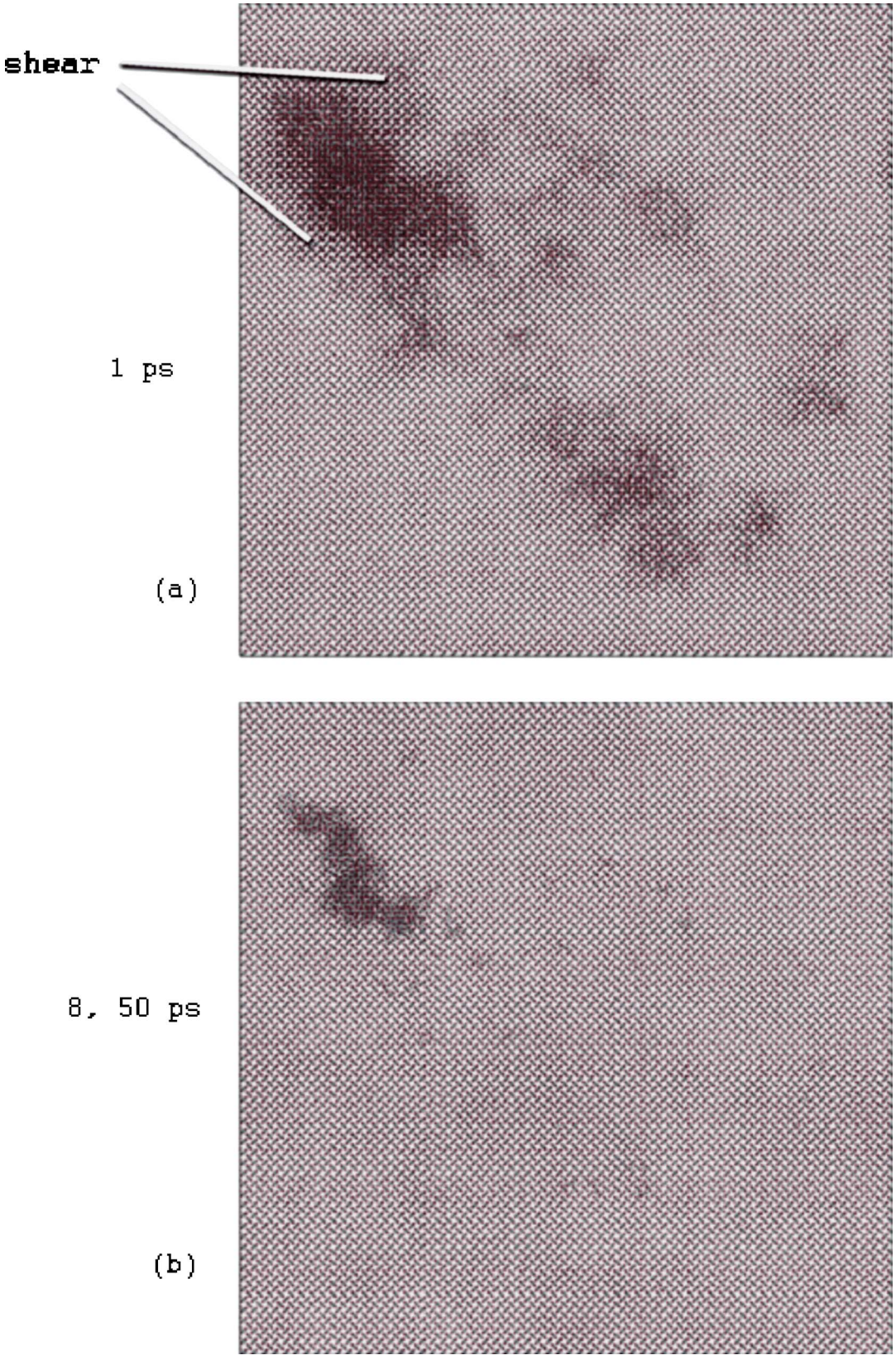

FIG. 3. (Color online) Radiation damage in TiO_2, showing the damage at its peak (top), and relaxed damage at the end of simulation (bottom). The size of MD simulation box is approximately 21 nm.

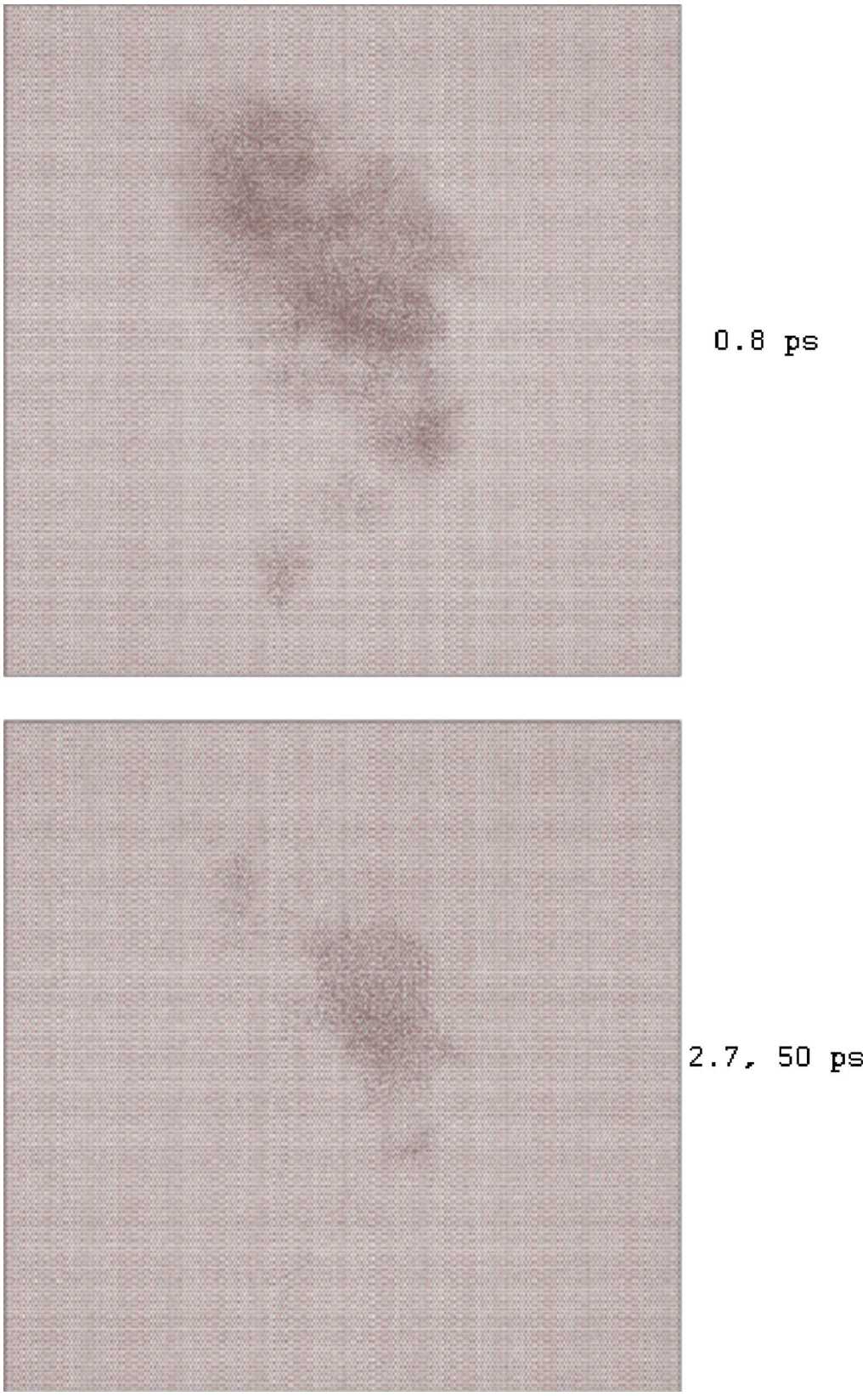

FIG. 4. (Color online) Radiation damage in $Al_2O_3^{(1)}$, showing the damage at its peak (top), and relaxed damage at the end of simulation (bottom). The size of MD simulation box is approximately 26 nm.

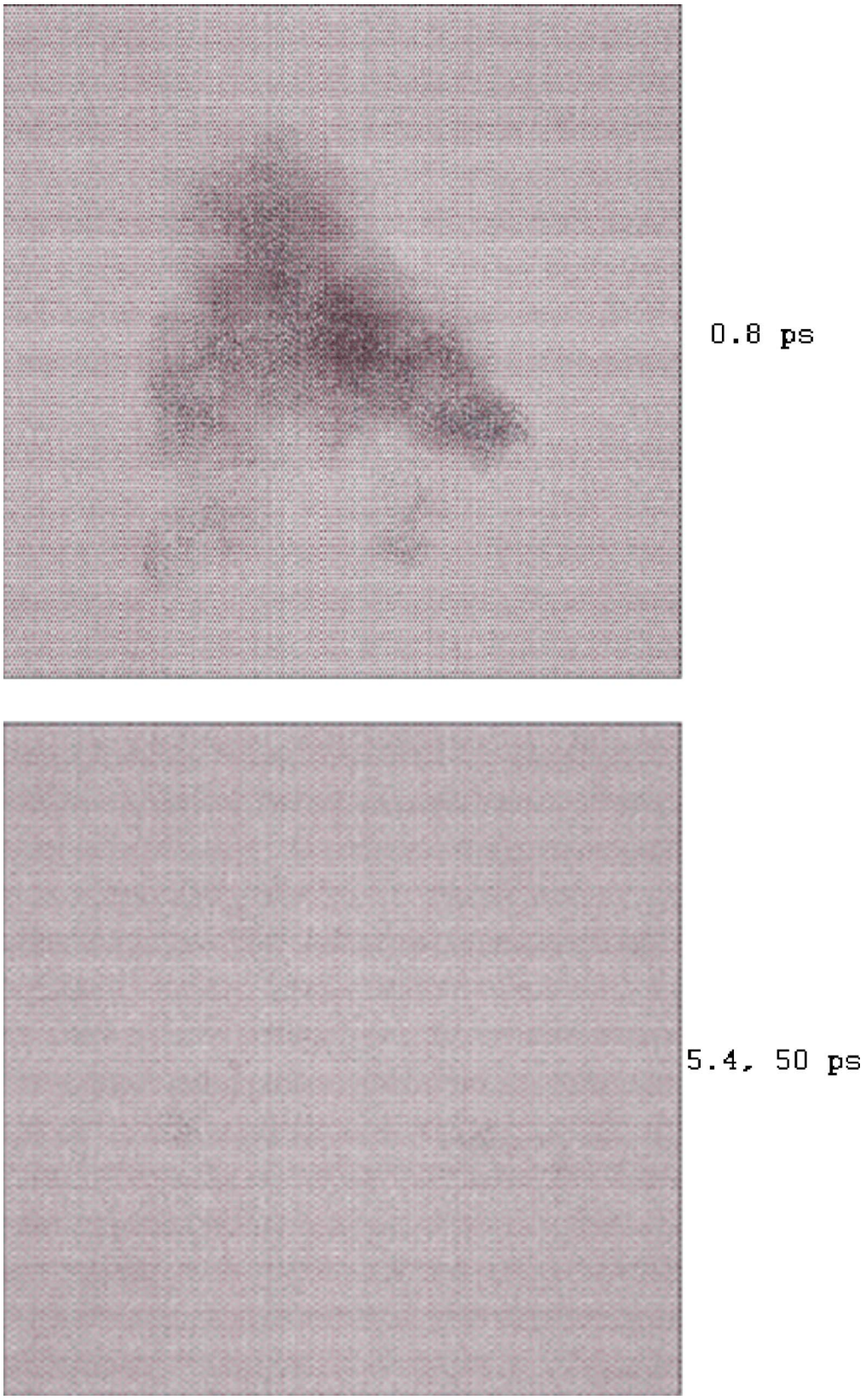

FIG. 5. (Color online) Radiation damage in $Al_2O_3^{(2)}$, showing the damage at its peak (top), and relaxed damage at the end of simulation (bottom). The size of MD simulation box is approximately 29 nm.

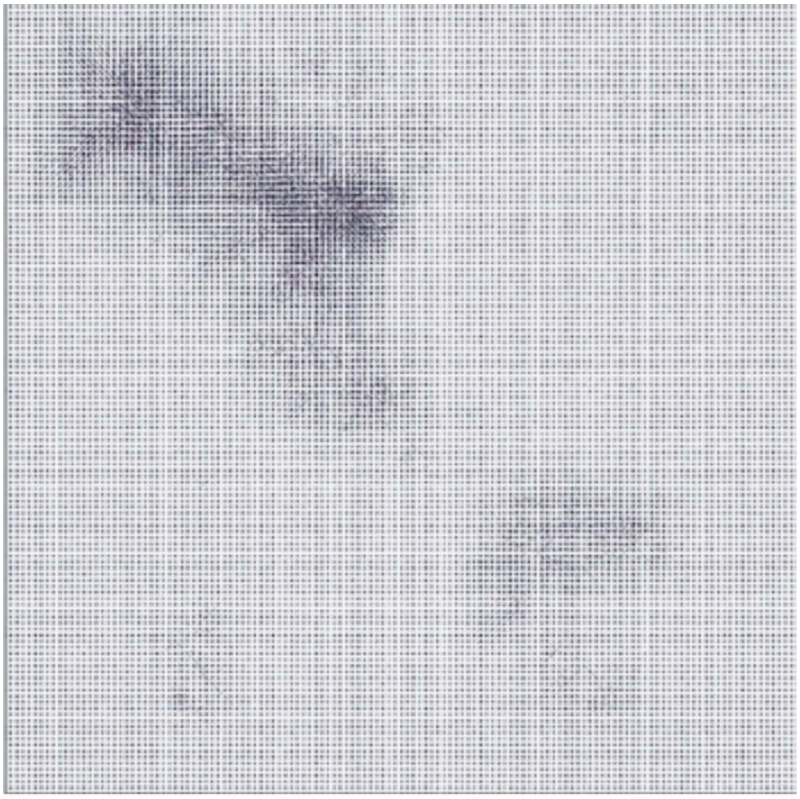

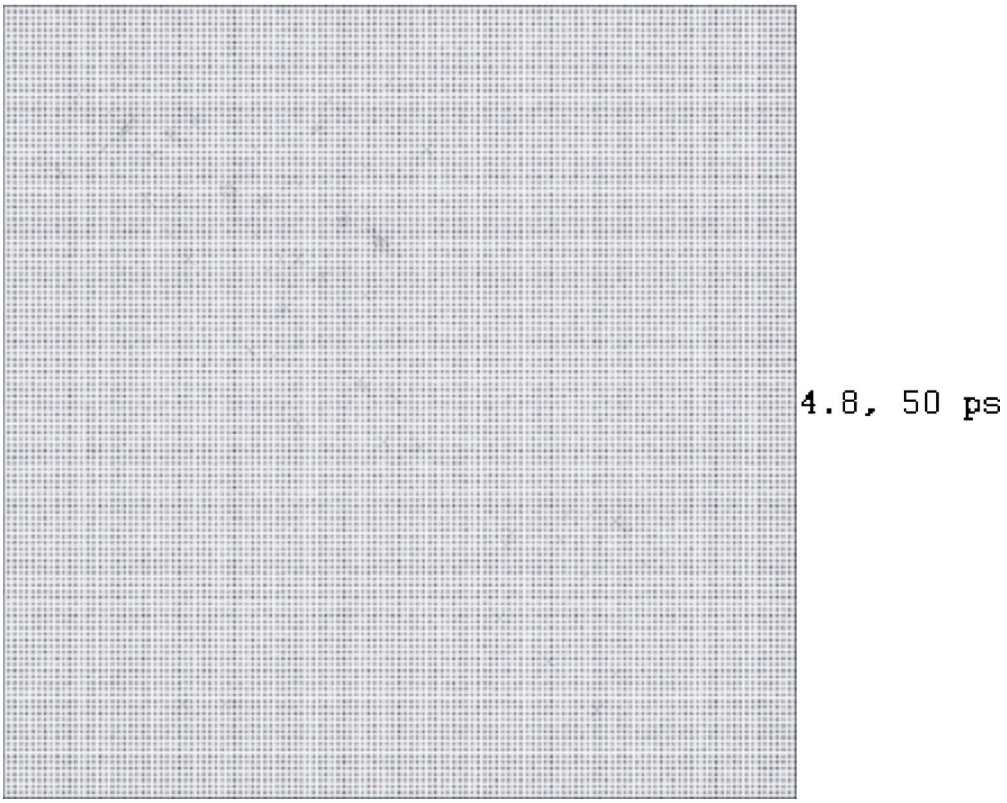

FIG. 6. (Color online) Radiation damage in MgO, showing the damage at its peak (top), and relaxed damage at the end of simulation (bottom). The size of MD simulation box is approximately 31 nm.

coordination and other defects, locally stressed regions and so on. The second note is related to quantifying the point at which the structure can be viewed as amorphous. The loss of the long-range order can be quantified by broadening of the Bragg peaks or by the loss of structure in the radial distribution function (RDF) at distances beyond the medium-range order (see below). Because these changes are continuous, this introduces an arbitrariness in defining the point at which the structure can be deemed amorphous. For these and other reasons, we consider the difference between the damaged structures in Figs. 1–6 in terms of the degree of structural damage, rather than the presence or absence of amorphous state, although we continue to use the term "radiation-induced amorphization," established in the field, in a sense that this state can be related to the loss of long-range periodicity.

As discussed above, the resulting damage is strikingly different along the series SiO_2, GeO_2, TiO_2, $Al_2O_3^{(1)}$, $Al_2O_3^{(2)}$, and MgO (see Figs. 1–6). We stress one important aspect of this difference. Materials with very efficient damage recovery as, for example, MgO, support the damage which can be discussed in terms of point defects, because these can be defined relative to the crystalline lattice, recovered after radiation cascade. However, such description of the damage is not adequate for materials like SiO_2 or TiO_2, because periodic atomic arrangement, destroyed by a cascade, is not recovered, and therefore point defects cannot be defined. We illustrate this point in Fig. 7, in which we contrast details of the damaged structure in TiO_2 and MgO from the simulation. We show the structures at about 50 ps, well after damage relaxation saturates in the MD simulation (see the time scales of damage relaxation, below). To highlight the high degree of structural damage in TiO_2, we show the interface between the crystalline lattice and the heavily damaged structure which shows no signs of periodicity [see Fig. 7(a)]. In MgO, on the other hand, the crystalline arrangement of atoms is recovered from radiation cascade to the extent that point defects can be defined. We illustrate this in Fig. 7(c). We find the region of MgO structure particularly rich in defects, and observe that even in this case, lattice is sufficiently recovered for point defects (or clusters of point defects in some cases) to be defined.

We further illustrate the high degree of damage in radiation cascade in TiO_2 by comparing the radial distribution function (RDF) of crystalline and damaged structure in Fig. 7(b). In comparing RDF, it should be first noted that RDF is insensitive to the difference between crystalline and amorphous structure not only in the short range, but also in the medium range. Indeed, RDF looks quite similar for both silica glass and its crystalline polymorphs up to 10 Å, reflecting the fact that there is not too much freedom in packing SiO_4 tetrahedra into continuous network, which results in the medium-range order present in glass.[19] Therefore the RDF peaks in the medium-range up to about 8 Å [see top of Fig. 7(b)] should not be taken as an indicator of the crystalline state. The important observation from Fig. 7(b) is the absence of peaks in RDF in the damaged structure after about 8 Å, in contrast with crystal. This suggests that the structure is highly damaged, and, if appropriate, can be considered amorphous in a sense that if a macroscopic sample consists of similar highly damaged regions, it possesses no long-range order. It should be noted that adding a large number of point defects to crystalline structure can also result in broadening of the peaks at longer distances and a RDF similar to that of amorphous structure. However, point defects cannot be discussed in cases when no crystalline arrangement is present in the damaged structure [see Fig. 7(a)].

This last point illustrates that in order to study radiation damage effects, the actual damage in the structure needs to be considered: point defects may be a reasonable description of the damage in materials like MgO, whereas this description is clearly not adequate for SiO_2, TiO_2 or any other material that can support permanent radiation cascades with high structural disorder. Indeed, our results show that in many important cases radiation damage is not a collection of point defects for the simple reason that there is no underlying crystalline lattice in the damaged region.

C. Comment on activation barriers

Damage recovery necessarily requires cooperative atomic rearrangements, with the energy barriers for damage recovery defined by the potential energy along the recovery path. These barriers are often referred to as activation barriers, in a sense that the probability to induce re-crystallization is $\propto e^{-V/kT}$, where V is the activation barrier.

We will discuss how V depends on MD input parameters, structure and interatomic interactions below, and here we note that V also can strongly depend on the degree of the damage. An interesting observation comes from damage recovery in TiO_2 (see Fig. 3). We find that highly disordered region shown in the left upper corner of Fig. 3(a) is due to primary U recoil, because the U atom stops not far from the bottom right corner of this region (recall that direction of the primary U recoil is from top left to bottom right). The damage in this region does not recover, resulting in the permanent damaged structure shown in Fig. 3(b). At the same time, during cascade development, the primary U recoil transfers large amount of energy to several lighter secondary Ti and O recoils. We find that these secondary recoils create the damage in other parts of the structure [see, for example, the lower part of the structure in Fig. 3(a)]. This damage is different from the U-created damage in one important respect, that the density of displaced atoms in the regions is smaller than that created by the primary U recoil [see Fig. 3(a)]. In other words, the damage is more dilute in these regions, which can be understood since the scattering cross sections of Ti and O atoms are smaller than that of the heavy U atom, resulting in smaller damage density. As follows from Fig. 3(b), this dilute damage recovers after several ps. This clearly shows that activation barriers for damage recovery can strongly depend on the degree of structural damage.

This observation helps understand experimental results that T_c is often higher if a material is irradiated by heavy ions, as compared to light ions. As we have seen, heavier ions produce denser cascades with higher activation barriers, and hence higher T_c.

This result reiterates the important point we made in the previous section: in order to study the response of materials

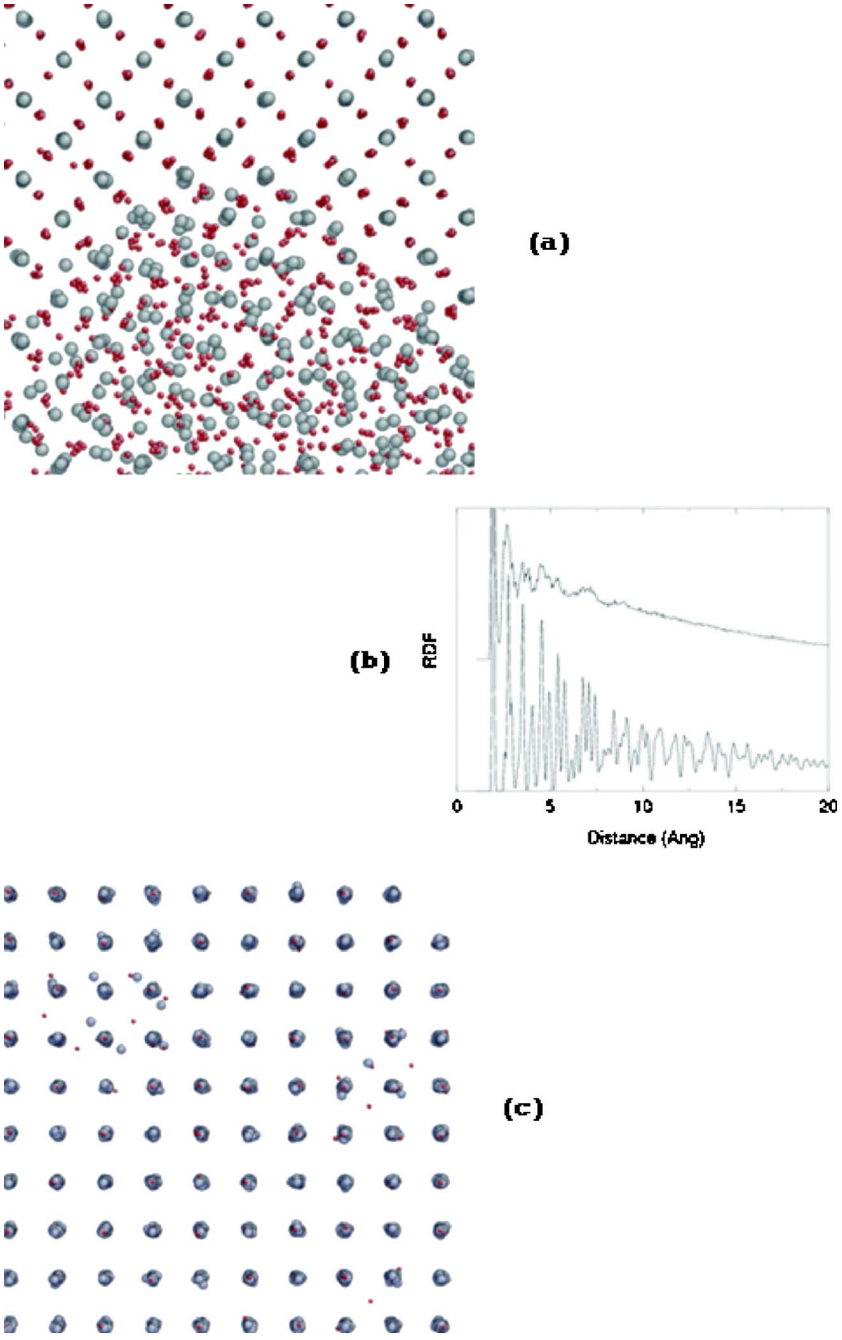

FIG. 7. (Color online) Difference between the highly damaged structure of TiO_2 and crystalline atomic arrangement in MgO. The structures are shown after about 50 ps in the MD simulation. We show (a) the interface between the crystalline arrangement and heavily damaged structure in TiO_2. The slice of the structure of approximately 3 nm thickness in direction perpendicular to the page is shown; (b) RDF calculated for TiO_2 crystal (bottom) and for the damaged structure (top); and (c) part of the damaged structure MgO, rich in point defects.

to displacive radiation, it is important to model the actual process of propagation of high-energy cascade and its recovery, because the activation barriers for damage recovery depend strongly on the actual structure of the damage.

III. TIME SCALES OF DAMAGE RECOVERY AND ELASTIC RELAXATION

Basing on Figs. 1–6, we can begin to discuss the question of what are the important time scales of damage recovery at room temperature. From Figs. 1–6 we observe that this time scale is set by several ps. A detailed comparison shows no difference between the structures immediately after radiation cascades at about 5 ps and structures at 50 ps (see Figs. 1–6). To quantify this point, we study how the amount of damage changes with time. The amount of damage is often quantified using the number of displaced atoms N_{disp}, defined as the number of atoms whose displacements exceed a certain distance. However, N_{disp} does not discriminate between materials that establish coherence with crystalline lattice (i.e., show damage recovery) and materials that support permanent damage. We therefore calculate the number of atoms which are "defect" relative to the crystalline frame of reference. An atom is considered an "interstitial" if it is closer to any of the crystalline positions (provided by the initial crystalline reference frame) than distance d and if there is already an atom that is closer to that crystalline site than d. A "vacancy" is defined as a crystalline position (again provided by

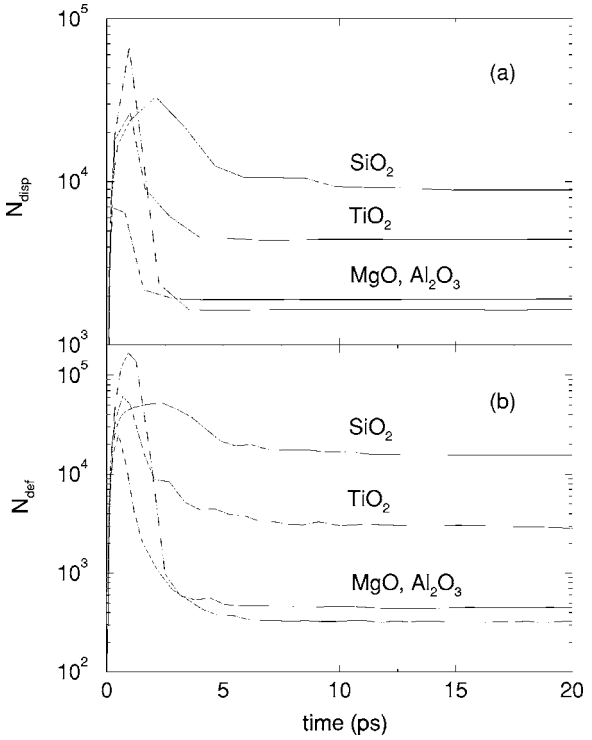

FIG. 8. Evolution of the number of (a) displaced atoms N_{disp} and (b) defects N_{def} in SiO_2, TiO_2, $Al_2O_3^{(2)}$, and MgO.

the initial crystalline reference frame) for which no atom exists that is closer to it than d. We calculate the number of defect atoms N_{def} as the sum of interstitials and vacancies for $d=0.75$ Å. To some extent, the definition of defect atoms arbitrary, however, it allows us to follow the dynamics of damage recovery. We plot N_{def} in Fig. 8, together with N_{disp}. We observe that in materials with and without damage recovery, N_{def} flattens out after about 5 ps, consistent the picture shown in Figs. 1–6.

It is interesting to note that a large contribution to the peak at $\sim 1-2$ ps in Fig. 8 is due to the atoms that create large elastic strain emanating from the radiation cascade into the crystalline lattice. These distortions can be observed in Figs. 1–6. The atoms creating these distortions are located in the interface between the regions of high structural disorder and surrounding crystalline lattice, and have displacements large enough to qualify as defects in our defect search algorithm. However, their positions, although highly distorted, preserve periodic arrangement of the lattice, and the corresponding deformation is reversible. We illustrate this point with the snapshot from the simulation of TiO_2 at 1 ps, in which we only plot the atoms that are displaced more than 0.75 Å (see Fig. 9). It is seen that highly damaged core of the cascade is surrounded by the displaced atoms which are arranged on the crystalline lattice. We note an interesting "ray"-shape pattern of atomic displacements that mostly run along the nearest Ti-O neighbor directions, projected on the plane. The elastic deformation due to these atoms does not contribute to the true structural disorder and is not associated with the process responsible for damage recovery. True structural damage is created in the core of the radiation cascade, and is characterized by high topological disorder (see Fig. 7). It is relaxation of this damage that governs damage recovery and resistance to amorphization.

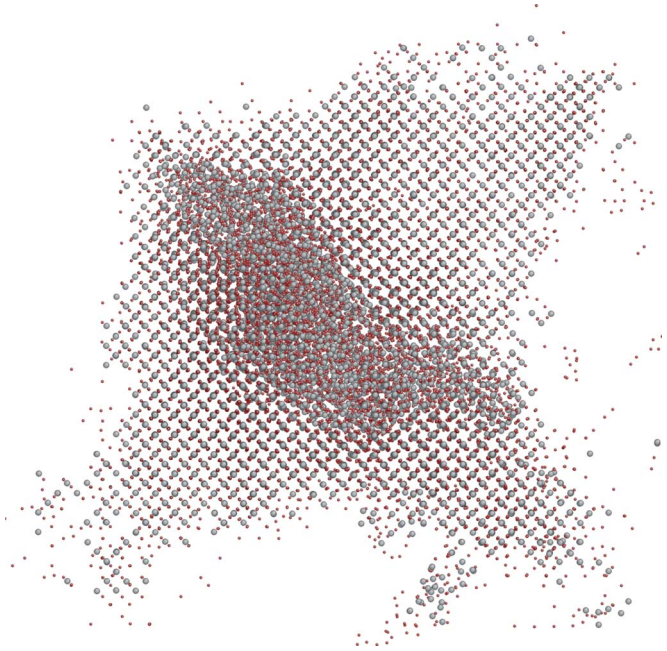

FIG. 9. (Color online) Snapshot from the simulation of TiO_2 at 1 ps. The direction of recoil is from top right to bottom left. Only atoms that are displaced more than 0.75 Å are shown. This snapshot shows that large number of displaced atoms around the highly damaged core are arranged on the crystalline lattice. Comparison with Fig. 3 shows that the accompanying elastic deformation is reversible. Note an interesting "ray"-shape pattern of atomic displacements that mostly run along the nearest Ti-O neighbor directions, projected on the plane.

It is interesting to observe further that the time scales of elastic relaxation (see Fig. 9 for the picture of elastic deformation around a radiation cascade) and of the recovery of the true structural damage are of the same order (see Fig. 8). For example, in MgO and $Al_2O_3^{(2)}$, N_{disp} and N_{def} saturate to their constant values at about 3 and 5 ps, respectively. In TiO_2, N_{disp} saturates at 3 ps [Fig. 8(a)], and is followed by somewhat longer relaxation of N_{def}, which saturates around 8 ps. The relationship between the two types of relaxation, reversible elastic deformation of the lattice around the radiation cascade (Fig. 9) and re-crystallization of the damage of high topological disorder (Fig. 7), can be the subject of future study.

As follows from Fig. 7, materials with efficient damage recovery (e.g., MgO and $Al_2O_3^{(2)}$) can support point defects at longer ~ 50 ps simulation times. Using temperature-accelerated MD method, it was found that migration and recombination of point defects in MgO can take place on a longer ms time scale.[3] Although these time scales are not accessible in the present simulations, we observe that remaining point defects constitute a very small part of the initially produced damage. Figures 1–6 suggest that it is stabilization or recovery of this damage, typically 5–15 nm in size, which is behind the phenomenon of resistance to amorphization. We have seen that if this damage recovers, it does so on the time scale of several ps.

One can ask if a material that remains damaged on the MD time scales may show damage recovery as a result of slow diffusive-type processes. Although such a recovery cannot be ruled out completely, we suggest that for materials with large activation barriers the recovery is probably not significant. At a qualitative level, this is supported by the general observation that materials that are readily amorphizable in the experiment (like Si and Ge) are also readily amorphizable in the MD simulations, i.e., do not show significant damage recovery on the MD time scales. One can also propose a quantitative argument in this respect. In (readily amorphizable) silicate, $ZrSiO_4$, MD simulations give the size of the damaged region produced by one event of about 4000–5000 atoms.[5,20] This is very close to what is measured in the diffuse x-ray scattering[21] and NMR experiments[22] on amorphous metamict samples (damaged by natural irradiation) of geological age. This suggests that in readily amorphizable materials with large activation barriers (see below), damage recovery beyond the MD time scales is not significant at room temperature. To demonstrate this further, we have simulated the damaged structure of SiO_2 at higher 1000-K temperature for approximately 40 ps, and found no damage recovery, consistent with large activation barriers.

IV. RESISTANCE TO AMORPHIZATION BY RADIATION DAMAGE

A. The challenge

We now discuss what affects damage recovery in classical MD simulations. For a given radiation cascade, activation barriers are defined by material's structure and its empirical potential. The effect of the material's structure is that, other conditions being equal, a highly coordinated structure generally tends to recrystallize more efficiently than a low-coordinated structure.[1] This idea dates back to the Phillips constraint theory of network glasses.[23] This theory assumes that in a solid with substantial covalent bonding, there exists the hierarchy of interatomic interactions, with short-range two- and three-body interactions considerably exceeding all other interactions. At temperature well below melting temperature, these interactions can be considered as mechanical constraints, in a sense that atomic motions obey the constraints of constant bond lengths and bond angles. Thus this picture maps interatomic interactions in a solid onto a mechanical network. A structure with the number of degrees of freedom equal to the number of constraints has the average coordination number of $\langle r\rangle = 2.4$. The case when $\langle r\rangle$ exceeds 2.4, corresponds to a "frustrated covalent network," which tends to recrystallize.[23] For the present study, this theory implies that if the potential is fixed and hence emulates the same degree of covalency in all materials (see below), an overcoordinated structure leads to more efficient recrystallization. For example, stishovite would show more damage recovery relative to quartz, provided both materials are simulated using the same potential. However, all five materials in this study use different empirical potentials, so the discussion of the structural aspects of damage recovery is not straightforward.

Because potential is fitted to material's structure, the two are not independent. Both (dependent) structure and potential also define a number of other properties, like elasticity, which may also be thought to be relevant for damage recovery.[24] Hence it is generally not clear how to disentangle the combinations of MD input parameters and pinpoint a particular relevant feature that is ultimately responsible for damage recovery. The absence of accepted model of resistance to radiation damage has made this task even more difficult. As a result, it has remained a challenge to establish the link between the observed damage recovery (or its absence) to the input parameters of the MD simulation. Instead, a large part of previous MD simulations concentrated mostly on the structures and types of radiation-induced defects, their kinetics and diffusion, effects of cascade and defect overlap, threshold displacement energies, etc.[1]

An interesting question, not explored before, is related to the fact that both experiments[1] and quantum-mechanical calculations[25] suggest that the nature of the chemical bond generally govern resistance to amorphization by radiation damage, as will be discussed in the next section. Classical MD simulations can simulate covalency explicitly by including three-body interactions in the force field. However, it is well known that the properties of materials with substantial covalency can also be reproduced very successfully with two-body interactions only, with SiO_2 and GeO_2 being common examples.[11,12] In our simulations, no three-body forces are part of the force field for any of the materials we study: all interactions are two-body forces. Although two-body forces can account for increased covalency by reducing the values of atomic charges, an important feature of covalency, the three-body forces originating from the high-energy cost involved in the deformation of electronic density distribution from its equilibrium polyhedral symmetry, is not included in the pair-potential force field explicitly. Yet experiments and quantum-mechanical calculations show that covalent contribution to bonding is strong in SiO_2 and GeO_2, somewhat decreased but still significant in TiO_2, whereas Al_2O_3 and MgO are regarded as highly ionic solids.[1] Hence it is interesting to ask how the picture of resistance in which the nature of the chemical bond is important can be reconciled with the results of this simulation, which reproduces experimental resistance correctly, but does not take bonding type into account explicitly. This point will be discussed in the next two sections.

B. Resistance to amorphization and the nature of the chemical bond

We have reviewed several factors affecting resistance to amorphization by radiation damage,[1] and discussed the important role played by the nature of chemical bond.[1,25,26] In this picture, higher covalency (ionicity) decreases (increases) resistance, through the increase (decrease) of activation barriers (it is implied here that a bond is "covalent" by a standard definition,[27] that there is strong directionality, as well as large value of electronic density between an atomic pair in a covalent case, as opposed to spherical symmetry and small value of electronic density between a pair in an "ionic" case).

If the chemical bond is covalent, an atomic pair lowers its energy through sharing electrons between two atoms, resulting in the binding energy as high as several eV. For damage recovery to take place, atomic rearrangements would involve breaking these stable electronic configurations (breaking short-range "covalent bonds") with associated high energy cost. If, on the other hand, the chemical bond is ionic, atomic rearrangements can proceed without the change in the electronic state of the atoms. As result, activation barriers increase with covalency of bonding. To reflect this, atomic rearrangements in covalent material are often said to be hampered by "hooking" of directional bonds, whereas in ionic material, ions "roll" with less energy cost.[28]

One can also discuss additional factors, related to the nature of the chemical bond, that affect resistance. A useful insight comes from the consideration of the potential energy landscape created by the short-range (covalent) and long-range (ionic) forces. The former results in the landscapes with many closely related minima, whereas the latter lead to landscapes with significantly fewer minima.[29] The damaged structure can stabilize in one of the many alternative minima in a material with dominating short-range covalent forces, whereas it is more likely to decay towards a crystalline minimum in a structure with dominating long-range electrostatic forces. Finally, in a material with high ionicity of bonding, the local recrystallization process is promoted by the need to compensate electrostatic charges, with an ion attracting oppositely charged neighbors and making the "defect" structures that consist of neighboring atoms of the same charge energetically unfavorable. This effect is absent in a covalent structure.

The review of experimental data of 116 materials shows a very good correlation between resistance and the nature of the chemical bond, with higher covalency and ionicity decreasing and increasing resistance, respectively.[1] This picture has recently been quantified by calculating the electronic structure of 36 materials.[25]

This general trend includes the binary oxides in the present study. Indeed, experiments and quantum-mechanical calculations show that covalent contribution to bonding is strong in SiO_2 and GeO_2, somewhat decreased but is still significant in TiO_2, whereas Al_2O_3 and MgO are regarded as highly ionic solids.[1] This decrease of covalency is consistent with increased resistance to amorphization of these materials in the same order. An interesting task now is to link this picture with the results of our classical MD simulations, which, as discussed above, do not take the nature of the chemical bond into account explicitly.

C. Resistance to amorphization in classical MD simulations: Activation barriers and three-body correlations

Large difference of damage recovery, as illustrated by Figs. 1–6, suggests that barriers to recrystallization V decrease substantially along the series SiO_2, GeO_2, TiO_2, $Al_2O_3(1)$, $Al_2O_3(2)$, and MgO. Having the knowledge of damage structure and interatomic interactions, one can attempt to calculate activation barriers. This meets the challenge for current transition states algorithms to handle systems with tens of thousands of atoms (see Fig. 8). Even if the distribution of activation barriers could be calculated for damaged structures shown in Figs. 1–6, it still leaves the question of why activation barriers vary from one material to another. It is therefore interesting to ask if one can trace the difference of V to the difference in interatomic interactions.

As heat is dissipated from radiation cascade, the interactions at equilibrium come into play and affect damage recovery. We note that common to all materials in this study is O-O interaction, and we find that damage recovery correlates with the steepness of O-O short-range interaction $F = \left|\frac{dE}{dx}_{x=r}\right|$, where E is the O-O Buckingham energy, $E = A\exp(-r/\rho) - C/r^6$, and r is the O-O distance. We find that $F \approx 1.5$, 0.6, 0.3, 0.2, 0.03, and 0.08 eV/Å for SiO_2, GeO_2, TiO_2, $Al_2O_3^{(1)}$, $Al_2O_3^{(2)}$, and MgO, respectively. It is seen that F decreases more than an order of magnitude as damage recovery progressively increases in these oxides in the same order (see Figs. 1–6).

We note that, although slightly, O-O distances vary along the series of oxides, which on its own might result in the decrease of F along the series of materials. However, we find that even if the same O-O distance is used to calculate F, the consistent decrease F is still observed in the same order, i.e., this trend reflects the difference in the steepness of the potential, as opposed to mere variation of nearest-neighbor O-O distances. We also note that in calculating F, we assumed that on average, the nearest-neighbor distance between O atoms in the cooling melt is the same as the corresponding distance in the crystal. This is equivalent to the existence of the same short-range order in a crystal and its melt.

We can discuss two aspects of relevance of F. First, F is related to the activation barrier for damage recovery. Generally, flat interatomic interactions give small activation barriers, hence the activation barriers should increase with the steepness of potential energy along the recovery path. This steepness has contributions from the steepnesses of Buckingham and Coulomb energy, δ_b and δ_c. Other conditions being equal (which may not always be the case, as will be discussed below), δ_b increases with F. Hence differences in F are reflected in the differences in total steepness of potential energy, provided that δ_c is not large enough to dilute the differences in δ_b. To show that this may not be the case, we calculate δ_b and δ_c as absolute values of the difference of Buckingham and Coulomb energy, respectively, of a small 1440-atom system due to a displacement of an O atom of 0.3 and 0.5 Å, averaged over 20 random directions. We find that for five materials studied here, δ_c/δ_b is about 0.1–0.8, therefore any difference in δ_b should be reflected in the total steepness of O-O interaction.

It should be noted that F is defined by O-O interaction that changes along the series SiO_2, GeO_2, TiO_2, $Al_2O_3^{(1)}$, $Al_2O_3^{(2)}$, and MgO. At the same time, A-O and A-A interactions change as well (in addition, Coulomb interactions also vary along this series due to the variation of atomic charges, although, as we have seen above, $\delta_c/\delta_b < 1$ for all materials). Because the variation of F along the series SiO_2, GeO_2, TiO_2, Al_2O_3, and MgO is inevitably accompanied by the variation of other interactions, the correlation of F with dam-

age recovery cannot be taken as an unambiguous demonstration that this correlation is the key to the observed behavior. Rather, we consider that the correlation between F and activation barriers is perhaps noncoincidental. Indeed, in quantum-mechanical picture of damage recovery, smaller covalency results in smaller energy barriers required to break short-range covalent bonds. Next, as follows from Figs. 1–7, empirical potentials give the result that activation barriers decrease along the series SiO_2, GeO_2, TiO_2, Al_2O_3, and MgO. If pair empirical potentials emulate the decrease of covalency through the decrease of activation barriers (recall that empirical potentials did not include three-body forces), then it is not unexpected that the decrease of the steepness of short-range O-O interaction, F, may manifest itself in the decrease of activation barriers. However, in the case of very different damage recovery in $Al_2O_3^{(1)}$ and $Al_2O_3^{(2)}$ (see Figs. 5 and 6), we can make a more definitive statement about the origin of this difference. This is because the difference of O-O interaction is the only substantial difference between the two cases. Indeed, the structure is obviously the same, as well as the charges on Al and O atoms, and (A,ρ,C) parameters of Al-O interaction are similar in both cases. Hence the correlation of damage recovery with F is not confounded by the inevitable variation of other parameters. Hence the dramatic increase of damage recovery in $Al_2O_3^{(2)}$ relative to $Al_2O_3^{(1)}$ can be correlated with nearly order-of-magnitude decrease of F more reliably.

Network-forming ability offers another way to discuss the correlation of F with resistance to amorphization. We have proposed[1,26] that a material is amorphizable by radiation damage if it can form disordered networks. The essential element of a network is the three-body force, and plays an important role in the formation of covalent glasses.[23] Recall that no three-body interaction is part of the force field of any materials in this study; however, three-body correlation can be estimated from the two-body forces by calculating the restoring force for distortion of the O-A-O angle. This restoring force is proportional to F, hence smaller F is related to smaller network-forming ability, consistent with increased damage recovery seen in Figs. 1–6. As in the case of activation barriers, this allows us to draw the parallel with the quantum-mechanical picture of damage recovery: in the quantum-mechanical picture, smaller F is related to smaller three-body interactions involved in distortion of interpolyhedral angles that define the symmetry of electronic density distribution. In classical MD simulations, smaller F gives smaller three-body O-A-O correlations and reduced network-forming ability.

On the basis of this discussion, one can ask a more general question of how covalency is modeled in MD simulations which use very common pair potentials, without three-body forces present. As discussed above, pair potentials on their own do not explicitly discriminate between a covalent and an ionic material. On the basis of the observed correlation of damage recovery with F, we suggest that such a discrimination can be implicit, in that an empirical force field of a covalent material, through larger F, results in a higher activation barrier as compared to an ionic one, and promotes network-forming ability through increased three-body correlations.

V. CONCLUSIONS

In summary, we find that MD simulations with empirical potentials generally reproduce experimental results of resistance to amorphization by radiation damage. This may enable one to use these simulations to predict experimental results. We have discussed the difference between the damaged structures along the series of several simple oxides. We have observed that (i) point defects can be fair representation of the damage in some materials, whereas this picture clearly fails for other materials that can support highly damaged structures, and (ii) the degree of structural damage can profoundly affect activation barriers for damage recovery. For these two reasons, we suggested that in order to study the response of materials to displacive radiation, it is important to model the actual process of propagation of high-energy cascade and its recovery.

We have observed that the phenomenon of resistance to amorphization mainly originates on the time scale of several ps, during which most of the damage recovers in resistant materials. On this time scale, we have observed two distinct relaxation processes, reversible elastic deformation around the radiation cascade, and recovery of the in-cascade damage of high topological disorder. Finally, we have found that damage recovery correlates with the steepness of interatomic interactions that affect activation barriers and three-body correlations, and discussed how these results can be related to the picture in which damage recovery is governed by the nature of the chemical bond.

ACKNOWLEDGMENTS

K.T. thanks K. Nordlund, R. Smith, J.C. Phillips, N.L. Allan, and M. Pruneda for discussions. We are grateful to EPSRC and NERC for support. Simulations have been performed on the HPCx parallel computers.

*Electronic address: kot@esc.cam.ac.uk

[1] For review, see K. Trachenko, J. Phys.: Condens. Matter **16**, R1491 (2004).

[2] R. Smith, *Atomic and Ion Collisions in Solids and at Surfaces* (Cambridge University Press, Cambridge, England, 1997); K. Nordlund, Nucl. Instrum. Methods Phys. Res. B **188**, 41 (2002); K. Nordlund, M. Ghaly, R. S. Averback, M. Caturla, T. Diaz de la Rubia, and J. Tarus, Phys. Rev. B **57**, 7556 (1998); D. J. Bacon and T. D. De la Rubia, J. Nucl. Mater. **216**, 275 (1994); A. Almazouzi, M. J. Caturla, M. Alurralde, T. D. de la Rubia, and M. Victoria, Nucl. Instrum. Methods Phys. Res. B **153**, 105 (1999).

[3] B. P. Uberuaga, R. Smith, A. R. Cleave, F. Montalenti, G. Henkelman, R. W. Grimes, A. F. Voter, and K. E. Sickafus, Phys.

Rev. Lett. **92**, 115505 (2004).
[4] T. Geisler, K. Trachenko, S. Rios, M. T. Dove, and E. K. H. Salje, J. Phys.: Condens. Matter **15**, L597 (2003).
[5] K. Trachenko, M. T. Dove, T. Geisler, I. Todorov, and B. Smith, J. Phys.: Condens. Matter **16**, S2623 (2004).
[6] K. Trachenko, M. T. Dove, E. K. H. Salje, I. Todorov, W. Smith, M. Pruneda, and E. Artacho, Mol. Simul. **31**, 355 (2005).
[7] S. X. Wang, L. M. Wang, R. C. Ewing, and R. H. Doremus, J. Non-Cryst. Solids **238**, 198 (1998).
[8] S. X. Wang, L. M. Wang, and R. C. Ewing, Nucl. Instrum. Methods Phys. Res. B **175**, 615 (2001).
[9] T. Hartmann, L. M. Wang, W. J. Weber, N. Yu, K. E. Sickafus, J. N. Mitchell, C. J. Wetteland, M. A. Nastasi, M. G. Hollander, N. P. Baker, C. R. Evans, J. R. Tesmer, and C. J. Maggiore, Nucl. Instrum. Methods Phys. Res. B **141**, 398 (1998).
[10] F. Li, M. Ishimaru, P. Lu, I. V. Afanasyev-Charkin, and K. E. Sickafus, Nucl. Instrum. Methods Phys. Res. B **166/167**, 314 (2000).
[11] S. Tsuneyuki, M. Tsukada, H. Aoki, and Y. Matsui, Phys. Rev. Lett. **61**, 869 (1988).
[12] T. Tsuchiya, T. Yamanaka, and M. Matsui, Phys. Chem. Miner. **25**, 94 (1998).
[13] M. Matsui and M. Akaogi, Mol. Simul. **6**, 239 (1991).
[14] G. V. Lewis and C. Catlow, J. Phys. C **18**, 1149 (1985).
[15] L. Minervini, M. O. Zacate, and R. W. Grimes, Solid State Ionics **116**, 339 (1999).
[16] J. Li, Modell. Simul. Mater. Sci. Eng. **11**, 173 (2003).
[17] See J. C. Dyre and N. B. Olsen, Phys. Rev. E **69**, 042501 (2004), and references therein.
[18] R. Zallen, *Physics of Amorphous Solids* (John Wiley and Sons, New York, 1983).
[19] F. J. Bermejo, C. Cabrillo, M. T. Dove, M. G. Tucker, K. Trachenko, D. A. Keen, M. J. Harris, and S. M. Bennington (unpublished).
[20] K. Trachenko, M. T. Dove, and E. K. H. Salje, Phys. Rev. B **65**, 180102(R) (2002).
[21] S. Rios, E. K. H. Salje, M. Zhang, and R. C. Ewing, J. Phys.: Condens. Matter **12**, 2401 (2000).
[22] I. Farnan and E. Salje, J. Appl. Phys. **89**, 2084 (2001).
[23] J. C. Phillips, J. Non-Cryst. Solids **34**, 153 (1979).
[24] J. Nord, K. Nordlund, and J. Keinonen, Phys. Rev. B **68**, 184104 (2003).
[25] K. Trachenko, M. Pruneda, E. Artacho, and M. T. Dove, Phys. Rev. B **71**, 184104 (2005).
[26] K. Trachenko, M. Pruneda, E. Artacho, and M. T. Dove, Phys. Rev. B **70**, 134112 (2004).
[27] N. W. Ashcroft and N. D. Mermin, *Solid State Physics* (Saunders College Publishing, Philadelphia, 1976).
[28] W. Huckel, *Structural Chemistry of Inorganic Compounds* (Elsevier, New York, 1951).
[29] D. J. Wales, Science **293**, 2067 (2001).